Quantitative study of the differences in mithocondrium distribution between DENV infected and mock cells

Juan Carlos Cardona and Juan Carlos Gallego-Gomez

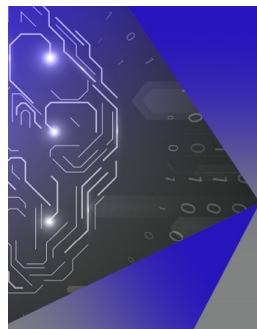View Online   Export Citation

ARTICLES YOU MAY BE INTERESTED IN

Computer vision system for evaluating the Schober's test
AIP Conference Proceedings **1747**, 090004 (2016); https://doi.org/10.1063/1.4954137

APL Machine Learning

Machine Learning for Applied Physics
Applied Physics for Machine Learning

Now Open for Submissions

Quantitative Study Of The Differences In Mithocondrium Distribution Between DENV Infected And Mock Cells

Juan Carlos Cardona [1,a)] and Juan Carlos Gallego-Gomez [2,a)]

[1] *Universidad del Atlántico, Barranquilla, Colombia.*
[2] *Universidad de Antioquia, Medelln, Colombia.*

[a)]Corresponding author: juancardona@mail.uniatlantico.edu.co

Abstract. The mithocondria distribution (MD) around nuclei is dynamically changing through clustering, fusion and fission of organelles [1], so the MD takes an appropiated form for each of the different cell functions [2]. Then it is expected that such distribution gets modified when the cell is under viral infection. To study such changes, several videos were taken through a set of live cell imaging experiments on cell cultures expressing fluorescent mithocondria of both: healthy (mock) and infected cells with Dengue Virus (DENV). The fluorescent organelles cluster in regions that shows up to be brighter where the MD is higher, then MD would be extracted from each frame as proportional to the brightness of the picture. Each experiment has follow standard protocols that provide approximately the same initial state for each cell of the same kind (mock or infected). As any studied cell starts from a different pattern of MD around the nuclei, it is expected for each one of those patterns to be equally likely, then the MD density can be approximated as the average of MD in each frame. Each MD has been modeled through a numerical function build as a two dimensional interpolation of the intensity levels, by using a bivariate b-splines method. Each cell has been modeled as an ellipsis, so the MD density function ρ is a function of the distance to the nuclei center r, the angle from major semi axis θ and time t. By carefully looking at $\rho(r,\theta,t)$ at fixed θ or fixed r (figure 1), it is clear that the distribution for infected cells has less defined clusters as shown by having more oscillations and lesser distance between peaks and background. Which means a more disorganized structure. This fact can be used to define a classifier for healthy or infected cells [3]. In this work, a proposal of a quantitative tool to measure the order or disorder on the MD is presented.

INTRODUCTION

We aim to study and characterize the differences found in mithocondrial distributions between cell cultures expressing fluorecent mithocondria. The procedure used to mantein the Vero epithelial cells is standard, and a full description can be found in other works [4, 5, 6]. Also, experimental details are provided in reference [3]. Brieftly: nine videos generated throught Live Cell Imaging (LCI) where studied; four were taken on mock cells (uninfected) cultures and five in infected cells cultures. The experiments last 12 hours, with images taken each $20m$. Cells are modeled under the assumption that cellular membrane and nuclei have elliptical shape, and both ellipsis are approximately aligned [7]. An autonomous segmentator was not available, so the image segmentation was performed by manual selection of four points into the nuclei of the target cell, and then applying the Hough transform [8] to fit an ellipsis. The cell membrane was assumed to be also an ellipsis, centered at the same point of the nuclei but with the length of each axis doubled. Only cells accomplishing the following criteria were taken into account: 1) the whole cell is present in all frames; 2) the nucleus is clearly recognized; and 3) the mitochondrial distribution does not seem to overlap with the neighbor cells. Under this criteria, a total of 4 mock and 7 infected cells where studied.

Each cell culture is prepared following the same standard protocols, then it is expected for each culture of the same kind to start frome the same initial state. However, the MD found in each cell at any given frame is different. As there is no reason for any initial particular MD to be more representative than the others, it is assumed than each one is a possible initial state occuring under some probability density distribution (PDD) valid for the given time. Such distribution can be approximated with the average of all the available known states at a give frame (time), and normalizing the area under PDD to one.

At the Live Cell Imaging experiment, the fluorescent mitochondria organelles are registered by the microscopy as a distribution of bright points, been more brilliant those places where the density of mitochondria is higher. The
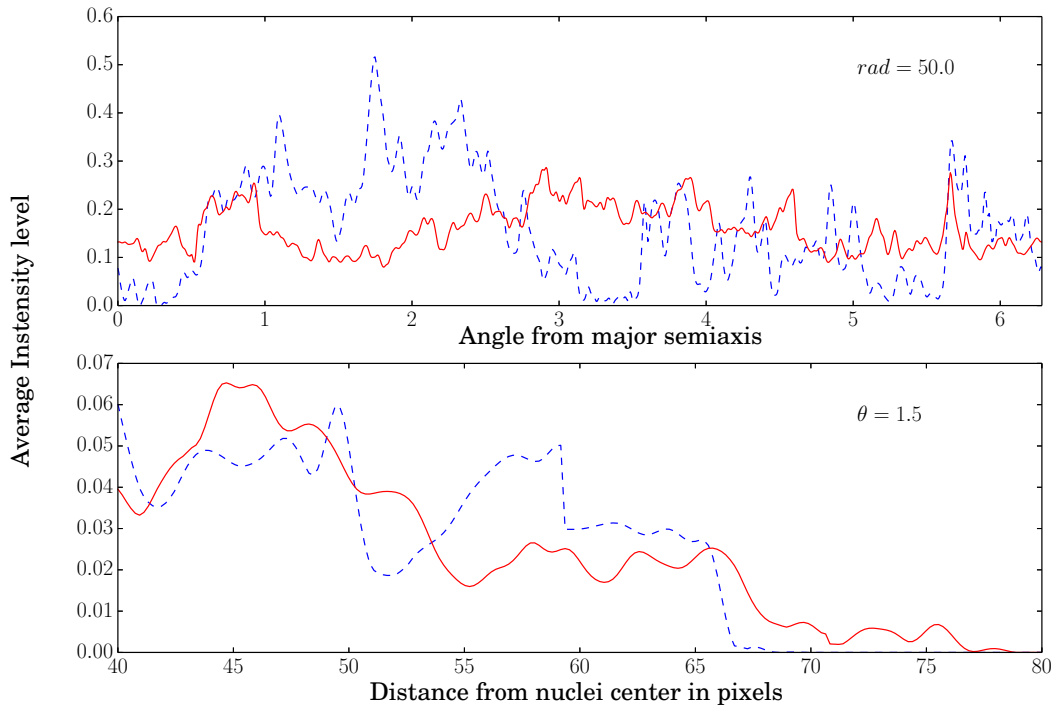
FIGURE 1. Probability density distribution PDD(r, θ, t) (color only in digital version) at $t = 0$, superior: at fixed distance $r = 50$ pixels, inferior: fixed angle $\theta = 1.5$ radians. Mock cells (blue dashed line) shows regions where the probability accumulates, which leads to the cluster formation. Infected cells (red continuous line) shows an angular distribution with high background, without clear recognizable clusters.

intensity levels registered in each picture depends not only on the MD, but also on the number of mithocondrias present in the cell, and even in the light spot. Those parameters can evolve in time or vary among different experimental setup. The influence of those factors on the average intensity must be avoided, so the intensity levels has been normalized to the maximum level present in each cell picture. Under this procedure, the intensity averaged is relative to the maximum on each picture, which is only dependent on the PDD determining the MD. Being so, the MD can be estimated to be proportional to the intensity distribution: $\rho(r, \theta, t) \sim I(r, \theta, t)$. Where r is the distance to the nuclei center, θ is the angle between the radial vector **r** and the major semi axis of the ellipsis, and t is the time when the image has been taken.

The formation of clusters in MD can be visualized through the average intensity graph (PDD) at any time (frame). At the surroundings of a cluster center the probability of finding a fluorescent organelle accumulates and must be noticeable higher than the background. In figure 1 the graph for the initial normalized PDD ($t = 0$) is shown for both kind of cells. The upper graph shows the PDD distribution for a fixed distance to the nuclei center (distance is measured in pixels) and lower graph shows PDD at fixed angle as a function of distance. In both graphs the reader would notice that the PDD function tends to be flatter for infected cells, in contrast with mock cells PDD where there are regions that holds high probability and regions with low probability of been occupied by an organelle. In the upper graph, the background probability for mock cells is near zero, but for the infected cells background is near 0.1. i.e., the peak-background distance is higher in mock cells. Small peaks are present in both PDDs, that can be due to random noise. The same analysis apply to the lower graph: there are regions where the probability of finding an organelle is clearly accumulated for mock cells, when for infected cells such probability seems to be spread. In both cases, the radial provability decay with the distance to the nuclear membrane, i.e., the organelles tend to be closer to the nuclei. It means that the distribution of mock cells has formed well defined clusters, and when the infection occurs, such organization is loosed and the organelles are not clustering properly.

QUANTITATIVE MEASURE OF THE DIFFERENT CLUSTER BEHAVIOR IN MOCK AND INFECTED CELLS.

The projection of the probability density distribution over given time and radius $\text{PDD}(r_o, \theta, t_o)$ is periodic in the angular variable, then fulfills all the required conditions to use the Fourier expansion and perform an spectral analysis. In Fourier basis, the representation of PDD looks as follows:

$$\text{PDD}(r_o, \theta, t_o) \quad = \quad \sum_{n=-\infty}^{\infty} \mathcal{A}_n(r_o, t_o) \exp(in\omega_o\theta), \tag{1}$$

$$= \quad \sum_{n=-N/2}^{N/2} \mathcal{A}_n(r_o, t_o) \exp(in\omega_o\theta) + \mathcal{E}_N. \tag{2}$$

Where the expansion coefficients $\mathcal{A}_n(r_o, t_o)$ depends on the time and the chosen radius, and $\omega = \pi/L$ is the basic frequency (in units of rad^{-1}). Computationally, the series must be truncated as shown in Eq. (2), where the series expands upon the truncation error $\mathcal{E}_N$ is small enough to be computationally negligible. The power of the n-th frequency term contribution to PDD is $\mathcal{A}_n(r_o, t_o)^2$. It gives an idea of how much of the function "energy" is carried out by the n-th term. The total "energy" of the power spectrum (PS) is $E = \sum_{n=-N/2}^{N/2} \mathcal{A}_n(r_o, t_o)^2$. Then, those frequencies that carry out the most of the PS energy are the most representatives. In the power spectrum, the contribution of random process tends to be evenly distributed over all the frequencies on the expansion, with its power tending to zero. As the spectra of a probability density distribution is bounded, the higher frequencies with small power represents noise in the signal (lower inset on figure 2.c), and in most cases can be safely removed. The noise in PDD for MD would come from small differences in the MD used to build it, and is responsible for the small peak-valley variations present in both, mock and infected cells MD.

The PDD for mock cells has a more complex structure than the one for infected cells, so the number of frequency terms in Eq. (2) with meaningful power contribution is expected to be larger on the PDD for mock cells (as shown in figure 2.c, with an enlargement on the upper inset). The power spectrum has been divided in two regions: the main region holding the major contribution to the power spectrum, involving all frequencies in the range $(-\omega_{cut}, \omega_{cut})$. And a tail region with all the frequencies such as $|\omega| \geq \omega_{cut}$. The main region is enough to describe the general PDD structure, holding more than 90% of the spectrum's energy and can reveal the location of clusters by removing from the PDD all noise coming from small differences in MD among cells an pure random noise. An example of the PDD expanded in terms of the main region is shown in the tick (black online) continuous line on figures 2.a and 2.b. Figure 2.a show the PDD for mock cells, where 4 regions of accumulated probability are clearly distinguishable, with a low background and large peak-valley distance. For the PDD of infected cells in figure 2.b the background is pretty high, and different from zero at all angles. Still there seems to be some regions where the probability is higher, but as the peak-valley distance is comparable with the background, there are not well defined clusters. A quantification measure of the difference between mock PDD and infected PDD has been computed under the following procedure: For each frame in mock and infected PDDs, 80 radii has been evaluated in the range $[40, 80]$ pixels. The starting radius is the average radius of the nucleus. For each radius, the power spectrum of $\text{PDD}(r, \theta, t_o)$ has been computed using the fast Fourier transform. The expansion size used was $N = 400$, which is enough to achieve convergence in both, mock an infected cells. This is shown in figure 2.a and 2.b respectively, where the full expansion of PDD (tick dashed line) is shown to overlap the original function. By direct inspection of the power spectrum it is found that a cutting frequency of $\omega_{cut} \sim 20 rad^{-1}$ is enough to define the main region at all frames at all radii, see figure 2.c. Then, the contribution of the tail to the energy of the power spectrum is computed as

$$\mathcal{T}_c = \frac{\sum_{n=\omega_{cut}}^{\omega_{max}} \mathcal{A}_n(r_o, t_o)^2}{E}. \tag{3}$$

Finally, the average over all radii of $\mathcal{T}_c$ gives a measure of the tail contribution to the whole frame. By comparing the tail contribution for mock PDD $\mathcal{T}_c^{(mock)}$ and infected PDD $\mathcal{T}_c^{(infe)}$, it was found that $\mathcal{T}_c^{(mock)} > \mathcal{T}_c^{(infe)}$ in the 97% of the frames.
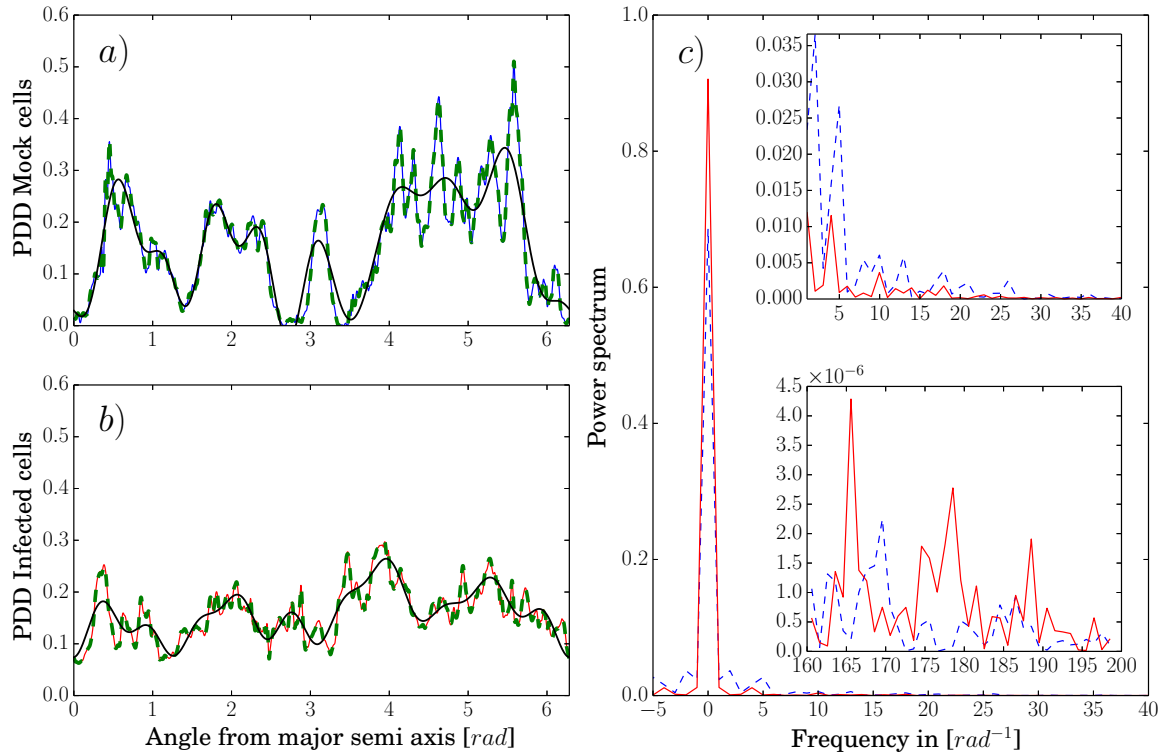
FIGURE 2. (color online) PDDs and power spectrum (normalized to the total "energy") at r_o = 47 pixels from nucleus center, and t_o = 20. a) Continuous line (blue): PDD for mock cells; Tick dashed line line (green): Fourier series approximation with 400 terms; Tick continuous line (black): Fourier expansion with only the 23 more significant terms. b) Continuous line (red): PDD for infected cells; Tick dashed line line (green): Fourier series approximation with 400 terms; Tick continuous line (black): Fourier expansion with only the 23 more significant terms. c) Power spectrum with 400 terms for mock (dashed blue line) and infected (red continuous line). Upper inset show the most meaningful frequency contributions. Lower inset shows the higher frequency zone (noise contributions).

CONCLUSION

The missing of cluster behavior on infected cells has been proven by a quantitative analysis of the PDD on the reciprocal Fourier space, where it was shown that PDD for infected cells has a lesser number of meaningful contribution terms on Fourier expansion. Which means a flater structure, showing less cluster behavior and a bigger random contribution.

ACKNOWLEDGMENTS

REFERENCES

[1]   L. L. Lackner, Curr. Opin. Cell Biol. **25**, 471 – 476 (2013).

[2]   J. Nunnari and A. Suomalainen, Cell **148**, 1145 – 1159 (2012).

[3]   J. C. Cardona, L. Ariza, and J. C. Gallego-Gomez, "A proposal for a machine learning classifier for viral infection in living cells based on mitochondrial distribution," in *Cell Biology - New Insights*, edited by S. Najman (InTech, Rijeka, 2016), pp. 3–25.

[4]   L. Padilla-S, A. Rodríguez, M. M. Gonzales, J. C. Gallego-G, and J. C. Castaño-O, Arch. Virol. **159**, 573–579 (2013).

[5]   M. Martínez-Gutierrez, J. E. Castellanos, and J. C. Gallego-Gómez, Intervirology **54**, 202–216 (2011).

[6]   A. T.-C. Elizabeth Orozco-Garca and J. C. Gallego-Gmez, "The role of cytoskeletal dynamics integrity in the effectiveness of dengue virus infection," in *Cell Biology - New Insights*, edited by S. Najman (InTech, Rijeka, 2016), pp. 143–162.

[7]   T. Zhao and R. F. Murphy, Cytom. Part A **71A**, 978–990 (2007).

[8]   R. O. Duda and P. E. Hart, Commun. ACM **15**, 11–15January (1972).